Optical detection of heterogeneous single molecule diffusion in thin liquid crystal films†

B. Schulz,‡ D. Täuber, F. Friedriszik,§ H. Graaf, J. Schuster¶ and C. von Borczyskowski*‖

Received 9th March 2010, Accepted 10th June 2010
DOI: 10.1039/c004042h

Lateral diffusion of three different dye molecules (terrylene and two perylene diimides) in 4 to 225 nm thin films of 8CB liquid crystals in the smectic-A phase has been investigated on a single molecule level. The influence of film thickness on tracer diffusion can be qualitatively modeled by a hydrodynamic approach. Molecular tracking experiments as well as fluorescence correlation (FCS) studies reveal the presence of diffusion dynamics which span a range of at least more than one order of magnitude in time, which is much larger than the reported anisotropic self-diffusion observed for 8CB bulk samples. We tentatively assign the heterogeneity to the formation of diffusion limiting domains on a micrometer scale within the 8CB films or at the interfaces.

Introduction

Liquid crystals are a prominent class of soft matter materials, which have found broad applications, even beyond liquid crystal cells.[1,2] The wide versatility is based on ordering phenomena which can be easily tuned by external fields or interfaces. For example, molecular ordering in thin smectic-A liquid crystals films is subject to external stress caused by antagonistic boundary conditions at the interfaces to solid substrates and air, respectively.[3] While *e.g.* the director of smectic-type liquid crystals is perpendicular to the liquid–air interface, the smectic crystalline structure crosses over to a nematic type for certain solid interfaces with the corresponding director being directed parallel to the solid–liquid interface. On the other hand, a highly corrugated surface, *e.g.* in porous silicon, acts as random field coupling to the order parameters of the confined phase and thus inhibiting the nematic to smectic phase transition in favor of the low-temperature metastability of the smectic phase.[4] Moreover, minimization of the free energy might be accompanied by the formation of self-organized structures such as the formation of hemi-cylinders[5] or focal conic domains.[6] Thin liquid crystal films and related structure formations are promising systems for various applications such as templates for photonic crystals.[7]

Many investigations related to the structure of thin liquid crystal films have been reported by AFM[8] and X-ray[5,9] techniques. However, to understand and manipulate ordering phenomena in thin films and at interfaces it is essential to also have access to the dynamics in such films at a molecular level. Translational and rotational diffusion are two of the most important dynamic properties. Diffusion in thin liquid crystal films and at interfaces have rarely been reported, as previous investigations have mainly probed liquid crystal bulk properties *e.g.* by NMR[10,11,12] or in pores by neutron back scattering[4,13] NMR results have been reported for bulk samples of 5CB smectic liquid crystals in pore structures with pore diameters of 10 nm[14] and for 8CB for transitions from isotropic to smectic phases within pores of 15 nm size.[15]

However, in pore structures it becomes difficult to systematically investigate the influence of film thickness on structure and diffusion, because with decreasing pore diameter the surface curvature and thus the solid–liquid interaction changes. Additionally, in pore structures it is nearly impossible to realize two different kinds of interfaces (solid–liquid or liquid–air). On the other hand, liquid crystal films with a thickness below 50 nm have due to sensitivity reasons not yet been investigated on plane substrates with respect to diffusion processes. To circumvent such an experimental short-cut (optical) probe molecules can be used as reporters of the liquid crystal film dynamics. Many recent experiments have shown that optical single molecule techniques are ideal tools to explore soft matter properties.[16,17,18,19] Spatially resolved single molecule experiments are superior to ensemble methods due to their sensitivity in revealing the influence of heterogeneities on the diffusion in ultrathin liquid films.[20,21,22,23] Usually fluorescent dye molecules with high photostability as well as with high quantum yields are used to probe the spatial distribution of static and/or dynamic properties of liquid films or confined liquids[16,19] *via* microscope techniques such as confocal or wide field optical microscopy. To the best of our knowledge, only a few experiments have been reported for single reporter molecules in liquid crystals.[24,25] Kawai *et al.* investigated diffusion of different diimide dye molecules in a parallel aligned nematic liquid crystal cell of about 5 μm height by fluorescence

Institute of Physics and nanoMA (Center for nanostructured Materials and Analytics), Chemnitz University of Technology, 09107 Chemnitz, Germany. E-mail: borczyskowski@physik.tu-chemnitz.de
† Electronic supplementary information (ESI) available: Additional experimental details. See DOI: 10.1039/c004042h
‡ Now at MPI for Dynamics and Self-Organization, Bunsenstraße 10, 37073 Göttingen.
§ Now at the University of Rostock, Institute of Physics, Dynamics of Molecular systems, Universitätplatz 3, D 18055, Rostock, Germany.
¶ Now at the Fraunhofer Research Institute for Electronic Nano Systems (ENAS), Technologie-Campus 3, D 09126 Chemnitz, Germany.
‖ Chemnitz University of Technology, Institute of Physics, Optical Spectroscopy and Molecular Physics, Reichenhainer Str. 70, D 09126 Chemnitz, Germany.

correlation spectroscopy (FCS). They found an anisotropic diffusion with nearly no dependence on the shape of the molecule. Lettinga *et al.* reported the diffusion of a rod-like virus in a smectic environment. They were able to observe a step-like motion of single emitters caused by the smectic layering.[26,27]

The few reported single molecule experiments show that diffusion of reporter molecules is strongly anisotropic, which in close relation with NMR detected self-diffusion has been assigned to diffusion parallel or perpendicular to the director of the liquid crystal. Experiments have also been reported for well defined orientations of liquid crystal layers in liquid crystal cells obtained by Rayleigh scattering[28] or FCS[24,25] and in free standing films by fluorescence recovery after photobleaching.[29] Though partly discussed, the influence of the interface and of self-organized structures still remains an open question, which is addressed in the present publication.

Additionally, besides the sensitivity restrictions inherent to NMR experiments in case of extremely small samples, the analysis of diffusion by NMR cannot be applied to frustrated liquid crystal configurations, as the strong magnetic field aligns the molecules destroying the alignment imposed by the interface. This argument also supports the concept that the analysis of reporter diffusion might be an alternative approach in case of thin films at interfaces.

Following the above perspectives, in this contribution we compare the results on diffusion dynamics in 4 to 225 nm thin 8CB liquid crystal films obtained by single molecule tracking to those obtained by FCS. We report on strongly heterogeneous diffusion in ultra-thin liquid crystal films, observed independently of the analytical approach, its relation to the film thickness and the properties of the interface (substrate). We use three types of reporter molecules which differ with respect to their ability to align along the liquid crystal structure. We tentatively assign the observed heterogeneity to intrinsic structural features of the liquid crystal films.

Experimental

Mesogen 4-n-octyl-4′-cyanobiphenyl (8CB, SYNTHON Chemicals) was used without further purification. 8CB has a smectic-A phase at room temperature, a transition to the nematic phase at T_{AN} = 33.7 °C and a transition to the isotropic phase at T_{NI} = 40.5 °C.[30] The films were prepared by spin-coating from a toluene (spectroscopic grade (>99.9%), Merck) solution containing ($\sim 10^{-10}$ mol l^{-1}) dye molecules. Depending on the film thickness this results in an upper limit of dye concentrations in 8CB between $\sim 10^{-7}$ mol l^{-1} (4 nm) and $\sim 10^{-9}$ mol l^{-1} (225 nm). The films where prepared on silicon substrates with either native oxide (Center for Microtechnologies, Chemnitz) or 100 nm thick thermally grown oxide interfaces (Center for Microtechnologies, Chemnitz). The film thickness was varied in a range between 4 and 225 nm by changing the concentration of 8CB in the toluene solution, and was controlled by X-ray diffraction. Experiments on a few 8CB layers by Bardon *et al.*[1] did not show evidence of dewetting processes. Our own AFM experiments on 225 nm 8CB also did not show dewetting for 8CB films kept at room temperature. Moreover, diffusion experiments did not indicate dewetting, since for all film thicknesses we observed "space-filling diffusion". Since the positioning accuracy is close to 50 nm, dewetted areas should be at this scale. We therefore believe that dewetting can be excluded.

We used two different perylene diimides (synthesis H. Graaf, TU Chemnitz) and terrylene (PAH Research Institute, Greifenberg, Germany) as probe molecules. The dye molecules are shown on scale in Scheme 1 in comparison to 8CB and together with the schematic smectic liquid crystal alignment. Details of the dye-8CB guest-host system are given in the ESI.†

One of the diimides (called orienting perylene diimide (o-PDI)) has been designed to align along the director of the 8CB smectic phase. The other diimide (called non-orienting perylene diimide (no-PDI)) did not show any alignment in the liquid crystal. Molecular alignment has been proven by varying the voltage applied to a nematic liquid crystal cell while detecting the related diimide fluorescence signal. We found an order parameter S = 0.7 for o-PDI and only S = 0.04–0.1 for no-PDI (for details see ESI).† In addition, we used terrylene, which, due to its comparatively small size, should not disturb the liquid crystal structure to a large extent and probably due to its elongated shape aligns along the director of the 8CB.

Two home-built single molecule fluorescence microscopes were used. The first one is a wide field microscope in *epi*-fluorescence mode operating with the 514 nm line of an Ar-ion Laser (Innova 70C, Coherent). The fluorescence of the sample is collected by a 100 × objective lens (Zeiss Epiplan Neofluar, NA = 0.9) and imaged on an electron multiplying CCD-camera (Andor iXon 885). Using a frame rate of 50 fps we were able to trace single molecule trajectories. The second setup is a confocal microscope equipped with a laser diode (465 nm, PicoQuant PDL 800D) and an avalanche photodiode (Perkin Elmer, SPCM-AQR-14) for single photon detection. The autocorrelation function was calculated by a correlator (ALV-5000 Multiple Tau Digital).

Analysis of single particle tracking is commonly performed *via* sampling mean square displacements (msd) along identified trajectories.[16,22,31] This approach is based on the two-dimensional Einstein-Smoluchowski equation

$$D_{msd} = \lim_{\Delta t \to \infty} msd(\Delta t)/(4\Delta t) \quad (1)$$

providing a relation between *msd* and the macroscopic diffusion coefficient D, valid in the long time limit. Since the translational diffusion in smectic-A liquid crystals is anisotropic,[11] one has to consider the time range of the anisotropy, and possibly the heterogeneous behavior of the diffusion.[32,33,34] Our analysis of the diffusion coefficients D_{msd} obtained from *msd* covers the time range of 0.1 to 3 s. An alternative approach to determine diffusion properties by single molecule tracking is to sample a large number of translational steps at time intervals of constant length and to investigate the related step distribution. One promising method is to sample the cumulative distributions of square displacements[35,36] or diffusivities[37,38] for fixed time intervals Δt. Diffusivities *di* are obtained by dividing the squared

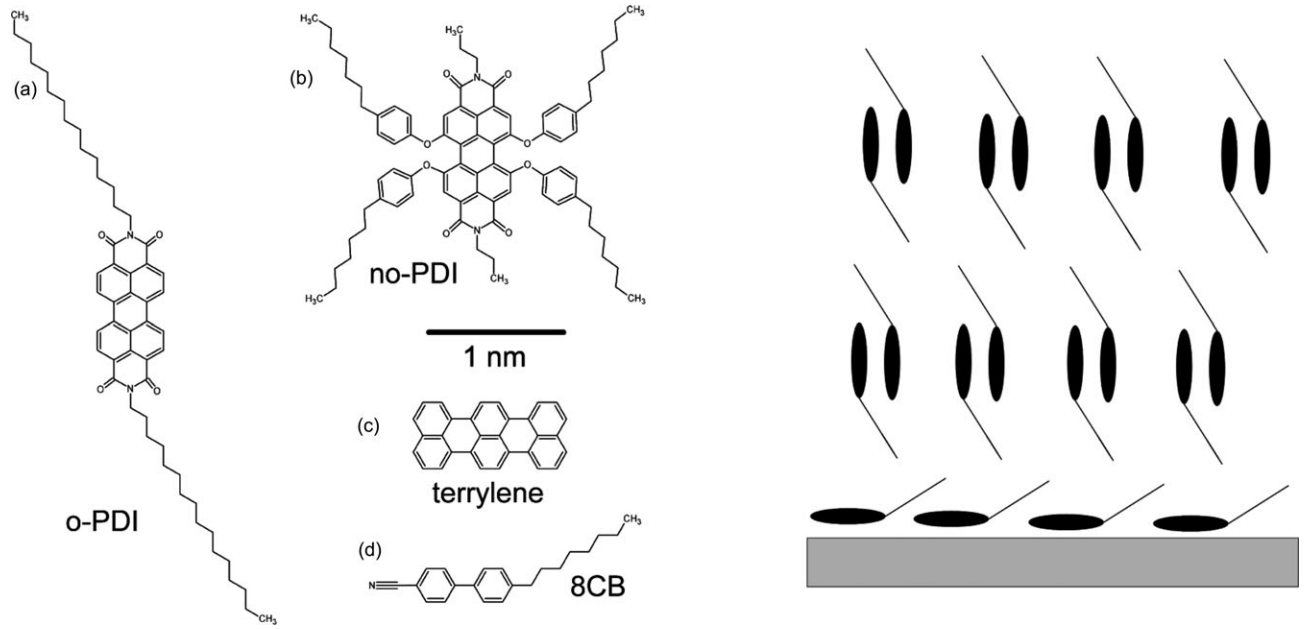

Scheme 1 Molecular structure of (a) o-PDI, (b) no-PDI, (c) terrylene and (d) 8CB. The right side shows the tentative liquid crystal structure at the interfaces with the substrate (bottom) and air (top).

displacements sd by $4\Delta t$. From these diffusivities time dependent short range diffusion coefficients $D_{di}(\Delta t)$ can be derived according to

$$D_{di}(\Delta t) = \langle di \rangle = \langle \mathrm{sd}(\Delta t)/(4\Delta t) \rangle \text{ (short: } D_{di}). \qquad (2)$$

Tracking experiments allow for a maximal temporal resolution of some tens of milliseconds, while FCS experiments yield a temporal resolution far below the millisecond range, limited only by the photon flux and the temporal resolution of the photodiode.

Results and discussion

The thinnest film was (4 ± 0.5) nm thick as detected by X-ray diffraction. This corresponds to 3 layers of 8CB, where the first monolayer is oriented planar to the quartz glass surface by physisorption[39] and is covered by one layer of 8CB-dimers (see Scheme 1). Such a conformation of 8CB has already been reported to form on native oxide interfaces for prewetting[1] and Langmuir films.[40] For all other film thicknesses the structure of the films is not known, except for silicon interfaces for which one obtains a random parallel alignment directly on the surface and a homeotropic alignment at the liquid–air interface.[3]

Dye fluorescence intensities of single emitters have been followed in time by single molecule tracking or FCS techniques. The assignment of the detected emission to single molecules is proven by the detection of fluorescence intermittency (blinking) which is a manifestation of truly single quantum objects (see ESI†).[54]

In the first step we analyze the dependence of the diffusion coefficient D_{msd} on the film thickness d. To proceed, we calculated D_{msd} determined from msd along each detected trajectory. We obtained slightly asymmetric distributions of D_{msd} values for each of the three dyes at various film thicknesses d (see Fig. 1a for no-PDI). Mean diffusion coefficients calculated from these distributions for 225 nm thick films are in all cases in the range of 2 $\mu m^2\ s^{-1}$ with a width of about 1 $\mu m^2\ s^{-1}$ (WHH). The results are shown in Fig. 1b as a function of film thickness for all three dye molecules. Here $\bar{D}_{msd}$ denotes the mean value from the above described distributions for each dye. We compare our results to a hydrodynamic model with no slip boundary conditions suggested by Lin *et al.*[41] who calculated the dependence of the diffusion coefficient of a sphere in a continuous medium in proximity to an interface. At first glance this model might seem not applicable to molecular diffusion in an anisotropic environment, but in the case of free standing films it has been shown that the diffusion of dye molecules only deviates from a continuum model film in a film thickness range of few molecular diameters.[29] The model predicts a slowdown of diffusion for very thin films. In single molecule experiments we only observe the diffusion projected into a plane parallel to the substrate. Additionally, a no-slip boundary condition does apply as the first monolayer is fixed to the substrate. Consequently we observe a slowdown in relation to the diffusion in the bulk according to

$$D/D_{bulk}\ (z) = 1\text{–}9/16\ (a/z), \qquad (3)$$

where a is the radius of the molecular sphere and z the distance of the molecule from the surface. As our exposure time is longer than the mean first passage time even for the film with the largest thickness of 225 nm, we only observe an averaging over the total film thickness.

Unfortunately we have no direct access to the distribution of dyes across the film thickness. Two limiting situations which may be envisaged are (i) a homogeneous distribution over the total film thickness and (ii) an enhanced concentration at the solid-8CB and 8CB-air interface. Enhanced dye concentration

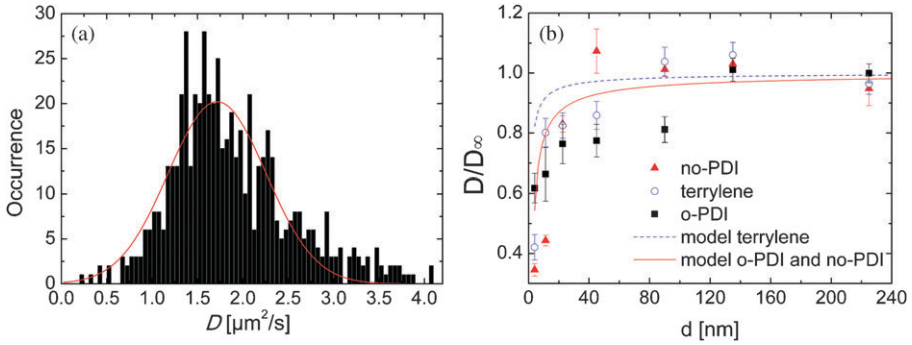

Fig. 1 (a) Distribution of D_{msd} of no-PDI calculated from diffusion trajectories for a 225 nm thick 8CB film on 100 nm SiO_2. The full line shows a Gaussian fit to the total distribution. (b) Normalized averaged diffusion coefficients $\bar{D}_{msd}/\bar{D}_{\infty}$ as a function of film thickness d for 8CB on 100 nm SiO_2. (Data for (○) terrylene, (■) o-PDI and (▲) no-PDI are also collected in Table 1).

at the LC–air interface would result with respect to the dye distribution in a "two-component" system with two related different diffusion coefficients. We show later with respect to FCS experiments, that if such two component systems with two related diffusion coefficients would be the appropriate description, it would need the assumption that the concentration of dyes is nearly the same at both 8CB interfaces, since the contribution of the two components is nearly independent of film thickness. Moreover, we have scanned the fluorescence intensities of PBI dyes over a 13 μm thick nematic cell (see ESI)† with a spacial resolution of less than 1 μm and did not find any intensity increments close to the substrate interface, but quite the opposite.

Although we cannot completely exclude the second assumption, let us in the following assume an equal probability of finding the molecules at all heights z above the surface. This leads to an integral of the locally slowed diffusion on the interval [a, d–a], with film thickness d and molecular radius a. The reason for this is that the molecule cannot approach closer to the surface than a and no further than d–a if it sticks completely inside the film. This leads to a slowdown of the diffusion dependent on film thickness and results in a scaled ratio of diffusion coefficients according to

$$D/D_{bulk}(d) = [d-2a-9a/16(\ln(d-a)-\ln(a))]/[d-2a]. \quad (4)$$

The comparison of this prediction to the experimental diffusion coefficients $\bar{D}_{msd}$ is also shown in Fig. 1b. The respective dye diameter a has been approximated by the arithmetic mean of the short and long molecular axis. Although our data do not fit the prediction perfectly, a general agreement is observed between experimental data and calculated ones for terrylene and no-PDI down to a film thickness of only a few molecular diameters. Above about 60 nm, $\bar{D}_{msd}$ becomes nearly independent of film thickness. We assign this to $\bar{D}_{\infty}$ (fictive bulk value). $\bar{D}_{\infty}$ depends only slightly on the type of dye molecule resulting in 1.8 $\mu m^2\ s^{-1}$ (o-PDI), 1.9 $\mu m^2\ s^{-1}$ (terrylene) and 2.2 $\mu m^2\ s^{-1}$ (no-PDI) though, according to the Stokes–Einstein formula, one would expect for terrylene a larger value than for PDI molecules. For the smallest molecule terrylene $\bar{D}_{\infty}$ is approached much faster than for PDI molecules. Though experimental findings and model predictions resemble each other, we however believe that the model is much too simple to reproduce all details of the related complex interface. This becomes more evident on inspecting the data for o-PDI. $\bar{D}_{msd}$ values show a notable deviation from the hydrodynamic model. In comparison to $\bar{D}_{\infty}$ they are significantly reduced up to 100 nm film thickness. This might be due to the particular behavior of o-PDI which aligns with the 8CB molecules. The first layer of 8CB is expected to align nearly parallel to the interface.[5] However due to the possibility of it being perpendicular in the next layers, the "effective" diameter a of o-PDI also changes along the distance z from the surface. A further possible reason for deviations from the hydrodynamic model might be related to the fact that the long axis of o-PDI (with completely stretched aliphatic chains) is about 50% longer than the diameter of a 8CB bilayer (see Scheme 1) and might therefore result in a larger effective radius.

The hydrodynamic model completely neglects specific interactions of the reporter molecules with the interface. However, from previous experiments we know [22,37,42] that dye molecules partly stick to the surface, *e.g. via* chemical (hydrogen) bonds to silanol groups,[16] which are to a certain extent always present at SiO_2 interfaces. Whether such bonds are also formed is unknown in the current case. The specific nature of immobilization is not of importance for the investigation of diffusion in the 8CB film, however a formation of bonds depends on the kind of dye molecule and the specific conditions at the interface. Bond formation would immobilize the dye molecules. The determination of diffusion coefficients D_{msd} from trajectories explicitly excludes trajectories with completely immobile diffusants. However, the cumulative distributions of diffusivities $C(di, \Delta t)$ take immobile diffusants into account. In Fig. 2 diffusivities di are collected for all three dye molecules in case of a 225 nm thick 8CB film at an averaging time of Δt = 20 ms. Since the focal depth is larger than 225 nm these measurements also provide information on molecules sticking at least for 20 ms to the interface. The observed distribution is a convolution of the real distribution with the positional resolution of the setup. Thus the "immobile" diffusants can be recognized as an extremely small D_{dio} in the $C(di, \Delta t)$ distribution. According to our positional precision of about 50 nm, these sticking events are related to $di < 0.06\ \mu m^2\ s^{-1}$. Inspection of Fig. 2 for very small di reveals that about 72% (terrylene) and 62% (o-PDI) but only 17%

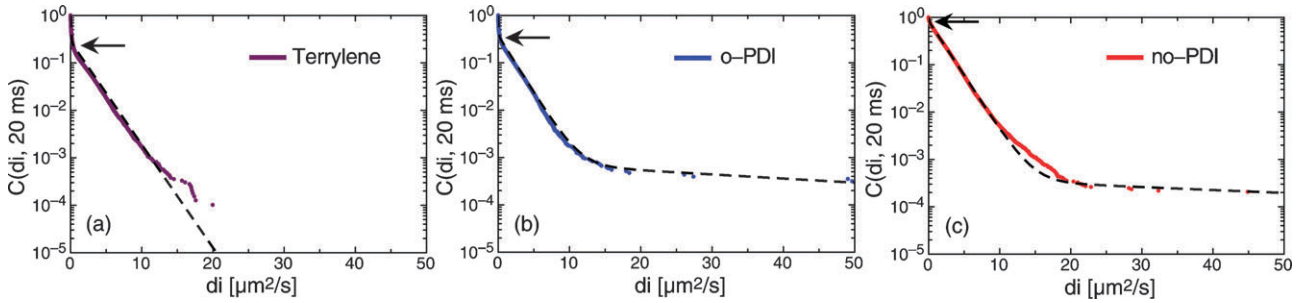

Fig. 2 Cumulative distributions $C(di, 20\ \text{ms})$ for (a) terrylene, (b) o-PDI and (c) no-PDI for 225 nm 8CB films on 100 nm SiO_2. Broken lines show a 2-exponential (a) and a 3-exponential (b, c) fit to the data. Horizontal arrows indicate the magnitude of the immobile component D_{dio}. The other fit results are collected in Table 1.

(no-PDI) are immobile (see arrows). In case that sticking events occur during the propagation along a trajectory, they apparently slow down the diffusion.

Determination of diffusion coefficients from trajectories or cumulative distributions of diffusivities is limited by the inherent time resolution given by the illumination time $\Delta t = 20$ ms. Therefore fast diffusion processes escape the experimental observation. This is more severe for the *msd*-based trajectory analysis, since the minimum total accumulation time for a trajectory is in the order of at least 1 s. Shorter time scales can be approached by the analysis of the cumulative distributions of diffusivities $C(di, \Delta t)$, where single lateral steps between two subsequent illumination times are registered. Following the recently outlined analysis[37,38] a (multi-)exponential fit to the distribution of diffusivities provides absolute values for the diffusion coefficients D_{di} and their relative contributions. Small D_{di} show up with a steep slope at small *di* values. Fig. 2 reveals that the diffusion of all dyes can in fact be approximated by two or three diffusion coefficients. As already discussed, the smallest one (D_{di0}) is in the range of 0.06 $\mu m^2\ s^{-1}$ and related to immobile molecules (see arrows in Fig. 2). In the following we completely neglect this component. The other two (D_{di1} and D_{di2}) vary by a factor of about 30. Independent of the analytical approach, the absolute values D_{msd} and D_{di} agree with each other within the experimental accuracy. Data from trajectories, diffusivities (and FCS) are collected in Table 1 for all dyes and a film thickness of $d = 225$nm. The contribution of the fast component D_{di2} (not evident from an *msd*-analysis of trajectories) is certainly underestimated, as a time resolution of 20 ms would allow only a few fast lateral steps to be observed[44] since, *e.g.* a molecule diffusing with 100 $\mu m^2\ s^{-1}$ would on average cover an area of 8 μm^2 during an exposure time of 20 ms, *i.e.* about 300 pixels on the CCD chip. On the other hand it takes, on average, only 13 ms to traverse 225 nm, *i.e.* our vertical film thickness.

To overcome this limiting time resolution, fluorescence correlation spectroscopy (FCS) is the method of choice to investigate fast dynamic processes *via* the intensity autocorrelation function

$$G_2(\tau) = \langle I(t)I(t+\tau)\rangle/\langle I(t)\rangle^2. \qquad (5)$$

For two-dimensional diffusion eqn (5) can be approximated[45] by

$$G_2(\tau) = 1 + A/(1 + \tau/\tau_D). \qquad (6)$$

τ_D is a characteristic time constant related to a diffusion coefficient by the size of the laser focus. At a film thickness of 225 nm two-dimensional diffusion is not strictly valid any more, since the focal length in z direction is in the order of 600 nm. Consequently, this results in a three-dimensional diffusion. However, the experimentally observed deviations are obviously not too large (see discussion later on). Therefore we restrict our further discussion on the two-dimensional approximation.

Fig. 3 shows as a typical example the intensity autocorrelation function $G_2(\tau)$ for no-PDI in 225 nm 8CB together with a fit according to eqn (6). It is immediately evident that the correlation function cannot be described by only one process. As shown by Hac *et al.*[46] improvement can be obtained assuming two dynamic processes according to

$$G_2(\tau) = 1 + A_1/(1 + \tau/\tau_{D1}) + A_2/(1 + \tau/\tau_{D2}). \qquad (7)$$

Now, as can be seen in Fig. 3, the agreement between experiment and a fit to eqn (7) is considerably improved. Even a better fit to the data is sometimes obtained by assuming anomalous (sub-) diffusion according to[47]

$$G_2(\tau) = 1 + A/[1 + (t/t_D)^{\alpha}], \qquad (8)$$

where $0 < \alpha < 1$.

In FCS only the change in the fluorescence signal within the confocal image is analyzed. This implies that all those effects

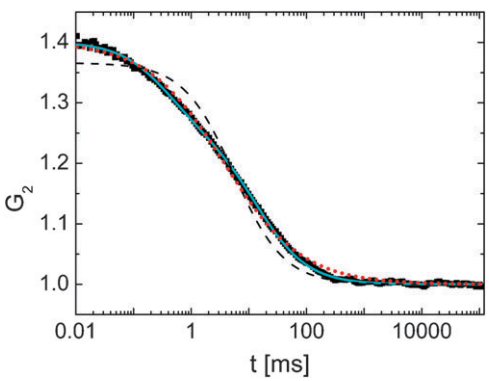

Fig. 3 FCS intensity autocorrelation function $G_2(\tau)$ for no-PDI in 225 nm 8CB on 100 nm SiO_2. Dashed black line: Fit with one diffusion coefficient (eqn (6)); full (cyan) line: Fit with two diffusion coefficients (eqn (7))); dotted (red) line: Fit assuming anomalous sub-diffusion (eqn (8)).

that influence the fluorescence intensity within the focal volume contribute to the correlation function (for example rotational diffusion[49] of the polarization of a dye molecule, blinking processes such as triplet intersystem crossing or photoinduced processes). For the different dye molecules due to their different sizes and intersystem crossing rates all these effects vary strongly. Moreover, intersystem crossing occurs for PBI molecules on a much faster time scale[52] than what is observed in the present FCS experiments. Photoinduced blinking is a rare event at least for PDI dyes. Therefore for o-PDI and no-PDI we approximate the autocorrelation function at least by two diffusion processes. Now τ_{Dn} can be related to a diffusion coefficient D_n by

$$\tau_{Dn} = w^2_{xy}/4D_n \quad (9)$$

w_{xy} is the lateral width of the laser focus and n equals to 1 or 2. The conclusion that FCS dynamics are related, at least partly, to translational diffusion, is strongly supported by the finding that the diffusion coefficients determined from FCS are in the same range (see Table 1) as those determined from trajectory and $C(di, \Delta t)$ analysis. For a 225 nm film the two diffusion coefficients D_1 and D_2 determined by FCS differ by a factor of 40–100. This ratio is somewhat higher than that obtained from $C(di, \Delta t)$ analysis (30). This fact can be easily attributed to the limited time resolution of $C(di, \Delta t)$, which results in an effective averaging (by increasing and decreasing the slow and fast) diffusion coefficients.[48] For the assumption of anomalous diffusion no diffusion coefficient can be calculated at all, as in this case only a transport coefficient can be defined.

Tracking msd and diffusivity data are quantitatively the same within experimental error. FCS data, however, provide as compared to tracking experiments similar absolute values for no-PDI but smaller ones for o-PDI and terrylene. We tentatively assign this finding to the fact that o-PDI (and terrylene) more strongly feel the orientation of the director of 8CB (see previous discussion). We thus find that experimental data from the three analytical approaches are in quantitative agreement with each other for no-PDI but differ for o-PDI and terrylene. We therefore conclude that for these two reporter molecules FCS is obviously also sensitive to processes additional to translational diffusion. While for no-PDI agreement between tracking and FCS data is in accordance with predominantly translational diffusion, the deviations observed for o-PDI and (terrylene) indicate that orientation-related processes have to be considered, to which only o-PDI and terrylene are sensitive due to their orientation with respect to the 8CB director. Such effects are caused by coupling of the reporter molecule to the fluctuations of the orientation of the 8CB director, which is well known for nematic liquid crystals,[50] and was also studied for 8CB.[51]

Comparing all our data on diffusion obtained from tracking experiments with those determined by NMR for self-diffusion in smectic 8CB crystals,[10] we find that for PDI there is an overall satisfying agreement (see Table 1) for the slow diffusion coefficient. However, there is a remarkable difference in the respective ratio (anisotropy) of the two diffusion coefficients found either by tracer detection or NMR. This is discussed in a later part of this paper.

In the following we discuss the FCS detected diffusion as a function of film thickness. In order to enable a comparison with data obtained from single molecule tracking we focus on the bi-exponential approach of the FCS data evaluation. In Fig. 4 we plot the correlation times τ_{D1} (Fig. 4a) and τ_{D2} (Fig. 4b) as a function of film thickness for o-PDI and no-PDI, respectively. The related amplitude ratios $A_1/(A_1 + A_2)$ are shown in Fig. 4c. All data have been obtained from fits according to eqn (7). For 8CB films thicker than $d = 80$ nm correlation times and amplitude ratios do not depend strongly on film thickness. The overall behavior, however, is more complex between 4 and 80 nm. This is the range to which both the hydrodynamic model and surface induced 8CB frustration apply. The hydrodynamic model predicts an

Table 1 Comparison of diffusion parameters[a]

Method	Reporter dye[b]	τ_{D1}/ms	D_1/μm^2 s^{-1}	τ_{D2}/ms	D_2/μm^2 s^{-1}
D_{msd}	o-PDI		3.1 (0.3)		
	no-PDI		2.7 (0.3)		
	terrylene		2.7 (0.3)		
C(*di*,20 ms)	o-PDI		2.7 (0.2)		75 (30)
	no-PDI		2.9 (0.2)		105 (40)
	terrylene		3.0 (0.2)		
FCS (2 diffusion coefficients)[c]	o-PDI	102 (35)	0.37 (0.3)	1.06 (0.2)	36 (11)
	no-PDI[f]	142 (5)	2.7 (1.2)	0.35 (0.05)	110 (30)
	terrylene[g]	105 (20)	0.36 (0.12)	2.89 (0.8)	13 (7)
FCS (anomalous)[d]		τ_D;τ[ms]	D[μm^2 s^{-1}]	α[i]	
	o-PDI	3.3 (0.5)		0.50 (0.03)	
	no-PDI	2.3 (0.4)		0.64 (0.03)	
	terrylene	1.5 (0.3)		0.50 (0.03)	
NMR[e]			$D_\perp$		$D_\parallel$
	8CB		13		28
	PDI[h]		4.3		9.3

[a] For the direct comparison the real diffusion constant in single-molecule tracking experiments is about 50% higher than the apparent diffusion constant.[32,43] Values in Table 1 are therefore scaled by a factor of 1.5 compared to those depicted in Fig. 1 and 2. [b] 8CB film thickness 225 nm on 100 nm SiO_2. [c] eqn (7) [d] and (9). [e] NMR results ref. 10. [f] Predominant intersystem crossing time at 1.5 K faster than 0.001 ms.[52] [g] Three-exponential fit with a short component of 0.016 ms, which is due to intersystem crossing.[53] [h] Calculated from NMR data with a by a factor of 3 effectively increased 8CB diameter. [i] The larger value of α for no-PDI as compared to o-PDI and terrylene indicates that diffusion is less heterogeneous.

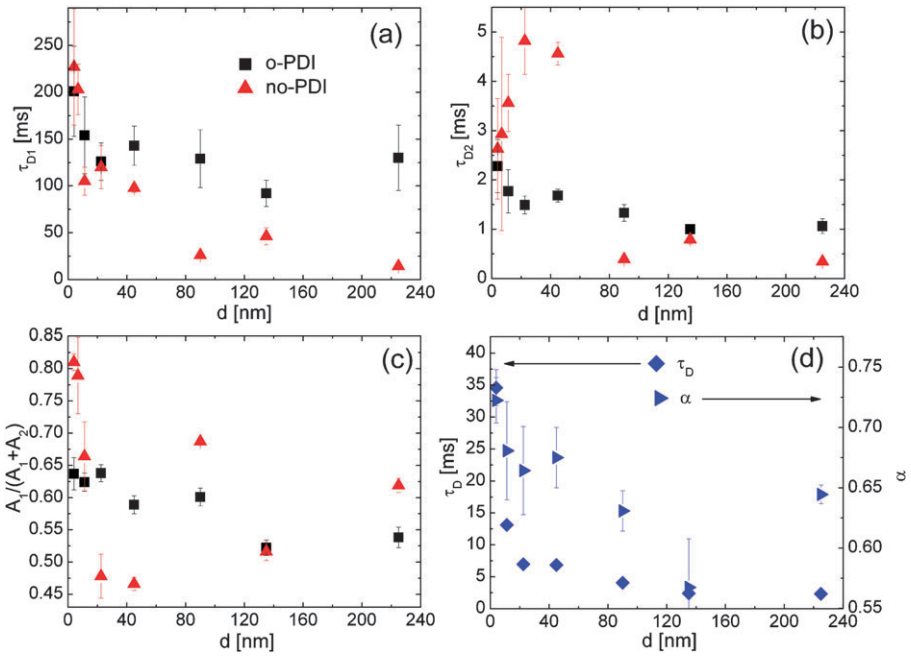

Fig. 4 Dependence of τ_{D1} (a) and τ_{D2} (b) and the amplitude ratio $A_1/(A_1 + A_2)$ (c) on film thickness for o-PDI (■) and no-PDI (▲); (d) dependence of time constant τ_D (◆) and α (▶) on film thickness for no-PDI.

increase of the diffusion coefficient with increasing film thickness d. This in turn corresponds to a decrease in the correlation times, which is in qualitative agreement with the experiments. At least above about 20 nm, both correlation times decrease continuously with increasing d. The range below $d = 20$ nm can be tentatively assigned to a range where 8CB molecules change their orientation with respect to the SiO_2 interface (see Scheme 1). While the long correlation time τ_{D2} still decreases continuously with increasing d, the short component τ_{D1} at least for no-PDI is obviously more sensitive to the specific conditions of the 8CB orientation. Since the behavior below 20 nm is complex and not yet understood, we leave it for further investigations and will, in the remaining part, concentrate on the thickness range above 80 nm.

Most important, the amplitude ratio of the two diffusion components is almost constant for $d > 80$ nm (see Fig. 4c). This observation is supported by a data evaluation postulating anomalous diffusion (eqn (8)) which also reveals a decrease of τ_D and α with increasing film thickness (see Fig. 4d and Table 1). Most of the related decrease occurs again between 4 and 80 nm. It is important to note that both approaches strongly indicate that diffusion dynamics does show heterogeneous behavior, almost independent of film thickness and the specific dye molecule.

Following all the above observations and arguments, we suggest that the hydrodynamic approach, already shown to be qualitatively valid when evaluating D_{msd} (slow diffusion), also describes the behavior of the fast diffusion coefficient. From the comparison of FCS data we conclude that the apparent diffusion of o-PDI is slower by about a factor of 2–5 as compared to no-PDI, while the contribution of the fast component is in both cases somewhat smaller than the one of the slow component. Most important, the observed heterogeneity of the diffusion process is influenced, but not predominantly caused by film thickness or frustration of 8CB layers close to the interface.

Summarizing up to this point, heterogeneous diffusion is observed for three different dye molecules by two different analytical approaches and is therefore an intrinsic property of the 8CB films. Generally it is known that (self-) diffusion in smectic liquid crystals is anisotropic as has been shown by NMR.[10] For bulk 8CB the ratio $D_{\parallel}/D_{\perp}$ of the two diffusion coefficients (diffusion parallel to the director respectively perpendicular to it[10]) at room temperature is close to 2 : 1.

As we have shown, o-PDI (and terrylene), to a certain extent, follow the orientation of the 8CB environment. Therefore we would also expect an anisotropic diffusion with a similar ratio of 2 for the two diffusion coefficients as has been observed in previous NMR experiments.[10]

However, according to our FCS experiments heterogeneity is much larger and in the range of 100 : 1 for o-PDI (and close to 50 : 1 and 40 : 1 for no-PDI and terrylene, respectively). Since the experimentally observed heterogeneity is much more pronounced than expected, we conclude that it is not caused by the intrinsic 8CB anisotropy of a well aligned liquid crystal phase. Inspecting Fig. 1a reveals that the distribution of diffusion coefficients obtained from msd is very broad and asymmetric. Though data statistics are too low for a definite conclusion, such a distribution would be in agreement with two diffusion coefficients differing by a factor of about two as is expected from NMR experiments.

Trajectory-type experiments only probe the projection of the diffusion into a plane parallel to the interface. In case that most of the 8CB smectic layers are nearly parallel to the substrate (see Scheme 1), only those trajectories are observable which include steps within the smectic plane ($D_{\perp}$). However, because of the projection, the diffusion perpendicular ($D_{\parallel}$) to

the smectic plane also contributes to the observed effective diffusion.[46] Similar arguments apply to FCS experiments.

Alternatively to an intrinsic anisotropy of the 8CB smectic crystal, the origin of the observed large heterogeneity might be related to a strong interaction of the diffusing dye molecules with the SiO_2 interface as has been observed for a variety of heterogeneous diffusion on SiO_2 interfaces.[16,49] We performed supporting experiments on substrates with native oxide. In that case the fluorescence signal is suppressed in the vicinity of the surface due to long range quenching processes induced by the Si substrate. Nevertheless, in that case we also observe a nearly constant ratio between the fast and the slow diffusion coefficient over the thickness range at least above $d = 80$ nm.

All the above arguments imply that some kind of lateral structure within the 8CB film might cause the heterogeneity. The typical length scale of such a postulated structure has to be in the range of the lateral focal diameter of the exciting laser, which is about 500 nm. First evidence of the existence of such structures is shown in Fig. 5. In this figure we compare the spatial distribution of diffusivities *di* for o-PDI and no-PDI which clearly show striking differences. Since o-PDI molecules and the related optical transition dipole moment μ along the long molecular axis nearly follow the orientation of 8CB, the fluorescence intensity varies according to the orientation of μ. As a consequence, the detection of lateral jumps with an orientation of μ perpendicular to the substrate, *i.e.* parallel to the 8BC director, is strongly suppressed. In case that "domains" exist with different orientations of the director relative to the substrate, this is "mapped" onto the fluorescence intensity distribution. Clearly, o-PDI doped 8CB films show "domains" on a length scale of a few μm, as detected by the distribution of "jumps" (see large blank "hole" in Fig. 5 left), while the randomly orientated no-PDI molecules do not show such "domains." We take this as an indication for the existence of the proposed spatial heterogeneity, though this is not yet an explanation of why the time scales of diffusion are so strongly different from each other.

Investigations of thin smectic 8CB films on flat crystalline MoS_2 show domains with a common orientation of the director. These domains have diameters in the order of microns.[9] This is not too far from what we observe experimentally in case of o-PDI. Even if such domains exist, they would induce an anisotropic diffusion typical of 8CB with a related ratio $D_{\parallel}/D_{\perp}$ of at most 2 : 1.[11] This ratio is, as already discussed above, by about one order of magnitude smaller than what we observe experimentally. However, when considering that such domains might be separated by a kind of "domain walls" strongly hindering diffusion of reporter molecules from one domain to the other, this might give rise to anomalous diffusion as would be consistent with the FCS data described according to eqn (8). Kawai *et al.* reported a single molecule detected broad distribution of the anisotropic ratio $D_{\parallel}/D_{\perp}$ in liquid nematic crystal cells,[25] which reaches ratios as large as 100 : 1 and is similar to our experimental results. On average, the reported anisotropy in the presumably highly ordered cell amounts to $D_{\parallel}/D_{\perp} = 5$. Additionally, it has been shown that the anisotropy is not caused by the asymmetry of the focal diameter due to the anisotropy of the refraction index of 8CB.[25]

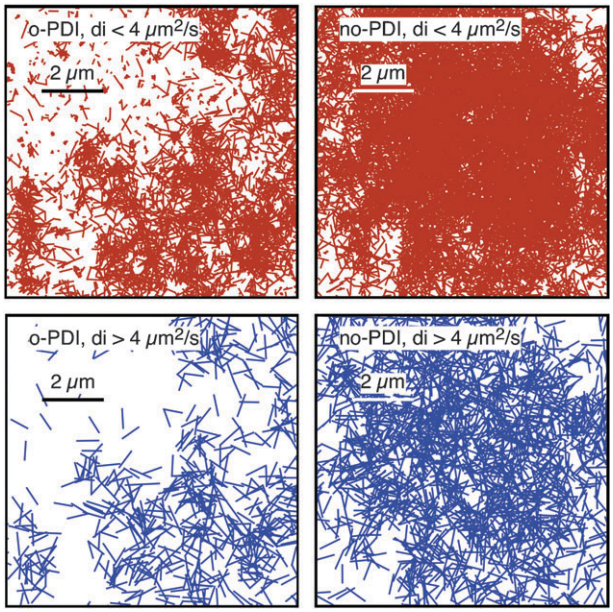

Fig. 5 Spatial distribution of diffusivities *di* for o-PDI (left) and no-PDI (right) for 8CB films with $d = 225$ nm on 100 nm thick SiO_2. For better visualization diffusivities smaller (larger) than 4 $\mu m^2 s^{-1}$ are shown in the two top (bottom) graphs. The size and shape of the laser illuminated spots is the same for both samples. Spatial o-PDI distributions show "holes" in the illuminated area (top left corner).

Alternatively, domain walls themselves might diffuse showing up in the diffusion dynamics as a fast component, since the slow component is at least for tracking experiments in closer agreement with NMR data. Clearly, this is a completely oversimplified picture, but nevertheless it demonstrates that diffusion limiting structures are of proper size in order to influence FCS based data. The alternative description of the FCS data by anomalous diffusion follows a similar interpretation. Finally it is worth mentioning that although most of our interpretation is based on the assumption of a homogeneous distribution of dye molecules across the film thickness, it would also be valid in case the dye molecules were (at comparable absolute amounts) distributed only in the two interfacing areas. The only difference is that in this case the identification of structure formation in 8CB would be restricted to the interfaces and no direct predictions can be made for the remaining film volume.

Conclusions

We investigated the diffusion of single reporter molecules in ultra-thin smectic 8CB (frustrated) liquid crystal films with a thickness between 4 and 225 nm. We could show that the diffusion of single reporter molecules can be qualitatively described by a continuum hydrodynamic model that predicts a strong influence of the interface with no-slip boundary condition for film thicknesses of some 8CB layers. We found that FCS data are sensitive to the type of reporter molecule. This is presumably due to the fact that those molecules which (partly) align with the 8CB director couple to related orientational fluctuations. Such fluctuations have been shown

by NMR experiments to take place on time scales in the range of ms and shorter.[50]

The diffusion is strongly heterogeneous over the total range of film thickness and differs considerably from the intrinsic anisotropic self-diffusion observed in NMR experiments. In fact, by comparing single molecule tracking and FCS experiments, we could show that the heterogeneous diffusion is an inherent property of the 8CB films either revealing two diffusion coefficients differing by a factor of about 50–100 or alternatively anomalous diffusion. We discussed several possible explanations and conclude that the observed heterogeneity is most likely related to the presence of domain structures in the range of μm or to a drastic increase of diffusion anisotropy in ultra-thin liquid crystal films. Under the present experimental conditions, we could not detect any ordered structures such as conic domains *via* optical reflection or fluorescence microscopy. The evaluation of further experiments is underway to investigate the influence of temperature or temperature cycling, since the formation of domain structures showed to be sensitive to thermalisation processes.[5,6]

Acknowledgements

We thank the DFG (Research Group FOR 877 (''From Local constraints to macroscopic transport'') for financial support. X-Ray data were provided by M. Kehr, TU Chemnitz. We enjoyed helpful discussions related to diffusion analysis with M. Heidernätsch, M. Bauer and G. Radons, TU Chemnitz.

Notes and references

1 S. Bardon, R. Ober, M. P. Valignat, F. Vandenbrouck, A. M. Cazabat and J. Daillant, *Phys. Rev. E: Stat. Phys., Plasmas, Fluids, Relat. Interdiscip. Top.*, 1999, **59**, 6808; M. Bras, V. Dugas, F. Bessueille, J. P. Cloarec, J. R. Martin, M. Cabrera, J. P. Chauvet, E. Souteyrand and M. Garrigues, *Biosensors and Bioelectrics*, 2004, **20**, 797; A. J. J. M. van Breemen, P. T. Herwig, C. H. T. Chlon, J. Sweelssen, H. F. M. Schoo, S. Setayesh, W. M. Hardeman, C. A. Martin, D. M. de Leeuw, J. J. P. Valeton, C. W. M. Bastiaansen, D. J. Broer, A. R. Popa-Merticaru and S. C. J. Meskers, *J. Am. Chem. Soc.*, 2006, **128**, 2336.
2 S. P. Meeker, W. C. K. Poon, 1, J. Crain, 1 and E. M. Terentjev, *Phys. Rev. E: Stat. Phys., Plasmas, Fluids, Relat. Interdiscip. Top.*, 2000, **61**, R6083.
3 V. Designolle, S. Herminghaus, T. Pfohl and Ch. Bahr, *Langmuir*, 2006, **22**, 363.
4 R. Lefort, D. Morineau, R. Guégan, M. Guendouz, J.-M. Zanotti and B. Frick, *Phys. Rev. E: Stat., Nonlinear, Soft Matter Phys.*, 2008, **78**, 40701.
5 J.-P. Michel, E. Lacaze, M. Goldmann, M. Gailhanou, M. de Boissieu and M. Alba, *Phys. Rev. Lett.*, 2006, **96**, 027803.
6 W. Guo and C. Bahr, *Phys. Rev. E: Stat., Nonlinear, Soft Matter Phys.*, 2009, **79**, 011707.
7 D. K. Yoon, M. C. Choi, Y. H. Kim, M. W. Kim, O. D. Lavrentovich and H.-T. Jung, *Nat. Mater.*, 2007, **6**, 866.
8 S. Bardon, M. P. Valignat and A. M. Cazabat, *Langmuir*, 1998, **14**, 2916.
9 E. Lacaze, J. P. Michel, M. Goldmann, M. Gailhanou, M. de Boissieu and M. Alba, *Phys. Rev. E: Stat., Nonlinear, Soft Matter Phys.*, 2004, **69**, 041705.
10 S. V. Dvinskikh, I. Furo, H. Zimmermann and A. Maliniak, *Phys. Rev. E*, 2002, **65**, 06170.
11 R. Y. Dong, *Phys. Rev. E: Stat. Phys., Plasmas, Fluids, Relat. Interdiscip. Top.*, 1998, **57**, 4316; M. Cifelli and C. A. Veracini, *Phys. Chem. Chem. Phys.*, 2005, **7**, 3412.
12 S. V. Dvinskikh and I. Furó, *Russ. Chem. Rev.*, 2006, **75**, 497; I. Furo and S. V. Dvinskikh, *Magn. Reson. Chem.*, 2002, **40**, S3.
13 R. Guégan, D. Morineau, C. Loverdo and W. Béziel, *Phys. Rev. E: Stat., Nonlinear, Soft Matter Phys.*, 2006, **73**, 011707.
14 E. E. Romanova, F. Grinberg, A. Pampel, J. Kärger and D. Freude, *J. Magn. Reson.*, 2009, **196**, 110.
15 M. Vilfan, T. Apih, P. J. Sebastião, G. Lahajnar and S. Žumer, *Phys. Rev. E: Stat., Nonlinear, Soft Matter Phys.*, 2007, **76**, 051708.
16 A. Honciuc, A. W. Harant and D. K. Schwartz, *Langmuir*, 2008, **24**, 6562.
17 N. Kahya, D. Scherfeld, B. Kirsten and P. Schwille, *J. Struct. Biol.*, 2004, **147**, 77.
18 P. Schwille, J. Bieschke and F. Oehlenschläger, *Biophys. Chem.*, 1997, **66**, 211.
19 C. Jung, J. Kirstein, B. Platschek, T. Bein, M. Budde, I. Frank, K. Müllen, J. Michaelis and C. Bräuchle, *J. Am. Chem. Soc.*, 2008, **130**, 1638.
20 J. Schuster, F. Cichos and C. von Borczyskowski, *J. Phys. Chem. A*, 2002, **106**, 5403.
21 J. Schuster, F. Cichos and C. von Borczyskowski, *Eur. Phys. J. E*, 2003, **12**, 75.
22 J. Schuster, F. Cichos and C. von Borczyskowski, *Eur. Polym. J.*, 2004, **40**, 993.
23 D. Hu and H. P. Lu, *J. Phys. Chem. B*, 2003, **107**, 618.
24 T. Kawai, S. Yoshihara, Y. Iwata, T. Fukaminato and M. Irie, *ChemPhysChem*, 2004, **5**, 1606.
25 T. Kawai, A. Kubota, K. Kawamura, H. Tsumatori and T. Nakashima, *Thin Solid Films*, 2008, **516**, 2666.
26 M. P. Lettinga and E. Grelet, *Phys. Rev. Lett.*, 2007, **99**, 197802.
27 E. Grelet, M. Letinga, M. Bier, R. Roij and P. Schoot, *J. Phys.: Condens. Matter*, 2008, **20**, 494213.
28 D. R. Spiegel, A. L. Thompson and W. C. Campbell, *J. Chem. Phys.*, 2001, **114**, 3842.
29 J. Bechhoefer, J.-C. Géminard, L. Bocquet and P. Oswald, *Phys. Rev. Lett.*, 1997, **79**, 4922.
30 T. Bellini, N. A. Clark, C. D. Muzny, L. Wu, C. W. Garland, D. W. Schaefer and B. J. Oliver, *Phys. Rev. Lett.*, 1992, **69**, 788.
31 M. J. Saxton, *Biophys. J.*, 1996, **70**, 1250.
32 M. Heidernätsch, *Master thesis*, TU Chemnitz, 2009.
33 A. Kammerer, F. Höfling and T. Franosch, *Europhys. Lett.*, 2008, **84**, 66002.
34 F. Höfling, T. Franosch and E. Frey, *Phys. Rev. Lett.*, 2006, **96**, 165901.
35 C. Hellriegel, J. Kirstein, C. Bräuchle, V. Latour, T. Pigot, R. Olivier, S. Lacombe, R. Brown, V. Guieu, T. Payaraste, A. Izquierdo and P. Mocho, *J. Phys. Chem. B*, 2004, **108**, 14699.
36 G. J. Schütz, H. Schindler and T. Schmidt, *Biophys. J.*, 1997, **73**, 1073.
37 D. Täuber, J. Schuster, M. Heidernätsch, M. Bauer, G. Radons and C. von Borczyskowski, *Diffusion Fundamentals Journal*, 2009, **11**, 107.
38 I. Trenkmann, D. Täuber, M. Bauer, J. Schuster, S. Bok, S. Gangopadhyay and C. von Borczyskowski, *Diffusion Fundamentals Journal*, 2009, **11**, 108.
39 B. Jérôme, *Rep. Prog. Phys.*, 1991, **54**, 391.
40 J. Xue, C. S. Jung and M. W. Kim, *Phys. Rev. Lett.*, 1992, **69**, 474.
41 B. Lin, J. Yu and S. A. Rice, *Phys. Rev. E: Stat. Phys., Plasmas, Fluids, Relat. Interdiscip. Top.*, 2000, **62**, 3909.
42 H. Graaf, M. Vieluf and C. von Borczyskowski, *Nanotechnology*, 2007, **18**, 265306.
43 D. Montiel, H. Cang and H. Yang, *J. Phys. Chem. B*, 2006, **110**, 19763.
44 D. Wöll, H. Uji-i, T. Schnitzler, J. Hotta, P. Dedecker, A. Herrmann, F. C. De Schryver, K. Müllen and J. Hofkens, *Angew. Chem.*, 2008, **120**, 795.
45 E. L. Elsonand and D. Magde, *Biophysics*, 1974, **13**, 1.
46 A. E. Hac, H. M. Seeger, M. Fidorra and T. Heimburg, *Biophys. J.*, 2005, **88**, 317.
47 P. Schwille, U. Haupts, S. Maiti and W. W. Webb, *Biophys. J.*, 1999, **77**, 2251.
48 M. Bauer, M. Heidernätsch, D. Täuber, C. von Borczyskowski and R. Radons, *Diffusion Fundamentals Journal*, 2009, **11**, 104.
49 A. V. Zakharov, D. Taguchi and M. Iwamoto, *Chem. Phys. Lett.*, 2008, **458**, 143.
50 R. C. Zamar, C. E. Gonzales and O. Mensio, *Braz. J. Phys.*, 1998, **28**, 314; O. Mensio, R. C. Zamar, E. Anoaredo, R. H. Acosta and R. Y. Dong, *J. Chem. Phys.*, 2005, **123**, 204911; H. Kneppe, F. Schneider and N. K. Sharma, *J. Chem. Phys.*, 1982, **77**, 3203;

H. Kneppe, F. Schneider and N. K. Sharma, *J. Chem. Phys*, 1982, **77**, 3203.
51 A. V. Zakharov, A. A. Vakulenko and J. Thoen, *J. Chem. Phys.*, 2003, **118**, 4253.
52 F. Lang, F. Würthner and J. Köhler, *ChemPhysChem*, 2005, **6**, 935.
53 F. Kulzer, F. Koberling, Th. Christ, M. Mews and Th. Basche, *Chem. Phys.*, 1999, **247**, 23; M. Vogel, A. Gruber, J. Wrachtrup and C. von Borczyskowski, *J. Phys. Chem.*, 1995, **99**, 14915.
54 F. Cichos, M. Orrit and C. von Borczyskowski, *Curr. Opin. Colloid Interface Sci.*, 2007, **12**, 272.

